Eur. Phys. J. B **4**, 13–23 (1998)

THE EUROPEAN PHYSICAL JOURNAL B

A phenomenology of boundary lubrication: the lumped junction model

T. Baumberger[1,a] and C. Caroli[2]

[1] Laboratoire de Physique de la Matière Condensée, Universités Paris VI, Paris VII et CNRS, École Normale Supérieure, 24 rue Lhomond, 75231 Paris Cedex 05, France
[2] Groupe de Physique des Solides, Universités Paris VI, Paris VII et CNRS, Tour 23, 2 place Jussieu, 75251 Paris Cedex 05, France

Received: 18 December 1997 / Received in final form and accepted: 26 March 1998

Abstract. We propose a phenomenological model of boundary lubricated junctions consisting of a few layers of small molecules which describes the rheological properties of these sytems both in the static, frozen, and sliding, molten, states as well as the dynamical transition between them. Two dynamical regimes can be distinguished, according to the level of *internal* damping of the junction, which depends on its thickness and on the normal load. In the overdamped regime, under driving at constant velocity v through an external spring, the motion evolves continuously from "atomic stick-slip" to modulated sliding. Underdamped systems exhibit, under given external stress, a range of dynamic bistability where the sheared static state coexists with a steadily sliding one. The frictional dynamics under shear driving is analyzed in detail, it provides a complete account of the qualitative dynamical scenarios observed by Israelashvili *et al.*, and yields semiquantitative agreement with experimental data. A few complementary experimental tests of the model are suggested.

PACS. 46.30.Pa Friction, wear, adherence, hardness, mechanical contacts, and tribology – 62.20.-x Mechanical properties of solids – 81.40.Pq Friction, lubrication, and wear

1 Introduction

Solid on solid friction has been a subject of renewed interest among physicists in the last decade, due to the concomitance of progress in several areas [1,2]. On the one hand, macroscopic experiments with submicronic resolution, performed on various materials (paper, PMMA, polystyrene), have permitted to investigate in detail the frictional dynamics of *multicontact interfaces*. These include fine measurements of static and dynamic friction coefficients, of their variations with, respectively, time and velocity, and extensive analysis of the stick-slip dynamics [3]. More recently, measurements of the d.c. [4] and a.c. [5] elastic interface response in the "static" regime give direct access to the pinning shear strength of the microcontacts and to the crossover between this regime and the sliding one. Multicontact interfaces, which we define as consisting of a large set of sparse, random regions of real contact of, typically, micrometric size, are the rule for contact between extended macroscopic bodies under apparent normal pressures smaller than, typically, $10^{-3}Y$ (with Y the yield stress of the material). Due to the fact that, in these situations, the distance between microcontacts is much larger than their size, elastic interactions between them are, to a good appoximation, irrelevant [6], and macroscopic friction results from the cumulative effect of individual pinning of each contact. It thus now becomes possible to extricate, from macroscopic data, information about the respective contributions of the various phenomena which have been known for a long time to contribute to solid friction – namely, statistical features of surface roughness on the micro and macro scales, elastic compression due to asperity relief, compressive plasticity, and shear strength and dissipation on the scale of what we will call the *junction*. By this is meant a very thin region along the real molecular interface of a microcontact between two asperities, probably of nanometric thickness, in which most of the deformation (and damage) under shear is localized. This region, in which most of the "frictional action" is believed to take place, contains in particular surface contaminants and lubricating molecules, if any.

On the other hand, the development of molecular tribometers [7,8], in particular the surface force apparatus (SFA) [7], has permitted to investigate extensively the mechanical behavior of systems composed of a few layers of lubricant molecules of various types, confined between atomically smooth mica surfaces, across a contact area of size in the $10\,\mu$m range. In this regime, called *boundary lubrication*, Israelashvili *et al.* [9,10] have studied extensively the frictional dynamics under steady shear

[a] e-mail: tristan@physique.ens.fr

driving, as a function of driving velocity, temperature, normal pressure and chemical nature of the lubricant, while Granick *et al.* [11] have investigated the response to an a.c. shear force as a function of amplitude level and frequency. A considerable body of experimental knowledge has thus become available, involving information about periodic and intermittent stick-slip regimes, dynamic friction force *versus* velocity in steady motion, delay times for restricking. On the other hand, the a.c. experiments give evidence that, in the "sticking" state, these junctions, when thin and compressed enough, behave as soft *viscoelastic solids.* At higher levels of deformation, of order 1, they cross over to viscous sliding. In parallel, numerical simulations [12, 13] have confirmed clearly that such highly confined layers solidify at temperatures much higher than the melting temperature of the bulk lubricant. They also show that, when submitted to an increasing shear stress σ, the frozen, pinned, lubricant, *melts under shear* for $\sigma = \sigma_M$. Moreover, in the cases studied, *dynamic hysteresis* is observed. Namely, when σ is decreased slowly from a value above σ_M, refreezing only occurs at a value $\sigma_L < \sigma_M$. This dynamic bistability (the existence of a range of values of σ where the layer can be either pinned or shear molten) has been correlated with the stick-slip dynamics.

It then appears very desirable to build a model of boundary lubricated friction which would encompass all the observed dynamical behaviors, at least in a phenomenological way. This would be useful in several respects. First, it would help rationalize and classify the existing data in a more systematic manner. Second, it would permit to correlate systematically the a.c. dynamical behavior at low and intermediate shear level of deformation with the sliding dynamics in the perspective of becoming able to directly infer one class of properties from the other. Finally, such modelling is necessary to start studying exactly how the physics of interasperity junctions manifests itself on the macroscopic level of a multicontact interface.

Carlson and Batista [14] have recently proposed a phenomenological model of boundary lubricated friction. This is based upon a constitutive relation describing the friction force on the sliding upper block of the SFA as a function of the block velocity and of a state variable θ, associated with the degree of melting of the layer. The friction law assumes the existence of a static threshold force, proportional to θ, below which the system is completely stuck. Above it, sliding takes place, giving rise to additional linear viscous dissipation. The state variable evolves with an overdamped dynamics with characteristic time τ for relaxation towards a stationary value varying from θ_{max}, at zero velocity, to θ_{min} for V above some critical value. That is, this model describes a system which, when it stops sliding, gradually transforms into a solid which remains infinitely rigid up to a stress value saturating at θ_{max}. Since it explicitly contains a dynamical transition under stress, it permits to account for

- stick-slip dynamics of the type observed by Israelashvili *et al.*;
- the existence of an upper critical value of the driving velocity, v_c, above which stick-slip disappears discontinuously and steady sliding settles in;
- the delay before regrowth of the static "stiction spike" observed in "stop-start" experiments, in which steady driving at $v > v_c$ is suddenly stopped, then resumed at the same velocity after a variable waiting time.

This model, although clearly useful to analyze sliding, suffers from two shortcomings. On the one hand, evaluating the values of the phenomenological parameters seems quite difficult, as they would have to be extracted from the full analysis of the highly nonlinear stick-slip dynamics. On the other hand, since the pinned state is assumed completely rigid, it can neither describe the a.c. viscoelastic response measured by Granick *et al.*, nor connect it with the sliding regime.

For these reasons, it appears useful to develop a more complete phenomenological model which describes the rheological properties of both the static, frozen, and sliding, molten, states, as well as the dynamical transition between them. The purpose of the present article is to propose such a model, for boundary lubricated junctions containing small molecules only. For reasons which will become clear shortly, we call it the "lumped junction" model.

In Section 2 below we formulate the basic equations and define two dynamical regimes, according to the level of *internal damping* of the viscoelastic lubricant layer. Responses under various types of shear driving are then analyzed in detail in Sections 3 and 4 which deal, respectively, with the overdamped and underdamped limits. In Section 5, we discuss our results in the light of existing experimental results, show that the underdamped version of the model provides a satisfactory semiquantitative account of existing observations, and suggest a few complementary experiments which could be of help for more quantitative comparison and provide further tests of the model.

2 The lumped junction model

It is clear from experiments that a complete rheological description of the lubrified joints must be viscoelastic, but

- essentially of the Kelvin type close to equilibrium ("frozen" state)
- of the Maxwell type beyond some stress threshold ("shear molten" state).

So, it cannot be expressed only in terms of the *velocity* of the upper surface of the joint (strain rate of the lubricant layer), it also has to involve the associated *displacement* (strain), knowing that, when the stress vanishes, the sliding (flowing) layer can solidify essentially on the spot.

Hence a pretty obvious formulation, which is summarized in the following equation. Call:

- M the mass of the joint (layer plus moving upper plate),
- x the position of its center of mass,

- K the stiffness of the external spring through which the external shear force is applied,
- $\rho(t)$ the position of the external end of the spring (pulling point),
- h the thickness of the layer,
- a^2 the area of the joint,
- η the viscosity of the layer in the linear regime, explored by Granick and coworkers by measuring the response of the static system to an oscillating shear force of very small amplitude.

We propose that the dynamical equation for the joint reads:

$$M\ddot{x} + \frac{\eta a^2}{h}\dot{x} + \frac{V_0}{b}\sin\left(\frac{x}{b}\right) + K\big(x - \rho(t)\big) = 0. \quad (1)$$

That is, we assume that the junction dynamics can be lumped into that of a single degree of freedom – translation of the center of mass along the direction of the applied shear force. A full description of the mechanical response of the system would of course involve all the (positional and conformational) degrees of freedom of the lubricant molecules. However, one may reasonably assume that, in the case of small molecules, the corresponding characteristic time scales are much smaller than those of the global (*e.g.* stick-slip) motion. The single degree of freedom reduction then corresponds to a quasi-adiabatic treatment of the fast internal degrees of freedom [15]. Such a process is equivalent to separating the layer mechanical response into an average total force, varying on the slow time scale of global motion, and a fast noise term, which we neglect at this stage. The non instantaneity of the fast internal dynamics gives rise to a retardation of the layer response, *i.e.* to a dissipative contribution (here modelled by the $\eta\dot{x}$ term in Eq. (1)) to the average force.

Clearly, such a separation of time scales becomes problematic in the case of long chain molecules, where configurational relaxation involves a broad spectrum of internal times the longest of which may become comparable with the global scale. The model can therefore only apply as such to the case of small molecules. We then make the ansatz that the internal stress σ on the joint is related to its strain x/h and strain rate $\dot{x}/h$ by:

$$\sigma a^2 = \frac{\eta a^2}{h}\dot{x} + \frac{V_0}{b}\sin\left(\frac{x}{b}\right). \quad (2)$$

In other words, we state that the joint is moving dissipatively in a periodic potential $V(x) = V_0\cos(x/b)$, which we assume for simplicity to be sinusoidal. If let to relax in the absence of external force, it will settle to equilibrium in one of the equivalent minima of the potential. The assumed multiplicity of pinning wells describes phenomenologically the possibility of resolidifying "on the spot" after sliding. Its seems natural to take for the space period $2\pi b$ of the pinning well structure that of the microscopic wall potential, *i.e.* b is of atomic order.

According to ansatz (2), close to equilibrium the linear mechanical response of the system is that of a viscoelastic *solid*. Namely, its linear response (as measured by experiments of the Demirel-Granick type [16]) is

$$\sigma = \eta\dot{\varepsilon} + G\varepsilon \quad (3)$$

with

$$\varepsilon = x/h; \quad G = \frac{V_0 h}{b^2 a^2}. \quad (4)$$

The internal viscosity η can be thought of as resulting from the dissipation associated with the above mentioned fast molecular processes. Here, we assume it to be frequency independent, in accordance with our assumption of a wide separation of time scales.

When writing equation (1), we have neglected noise. We will come back to this later. For the moment, our aim is to try and classify the possible dynamical regimes of a system obeying this deterministic equation, which is simply that of the driven damped pendulum. It has been extensively studied analytically and numerically, and its various regimes have been classified, in particular in the context of studies of the dynamics of Josephson junctions, where it corresponds to the "lumped circuit model". We are therefore in the comfortable position where we can draw extensively upon previous results, which we will now transcribe into our language. We follow especially closely the article of Ben Jacob and Imry [17]. We give in the Appendix a table of correspondence between the variables and parameters of our mechanical problem and those of the Josephson one.

In the absence of external force ($K = 0$) equation (1) involves two times:

- the inertial time associated with the internal inertial frequency of the joint, defined by:

$$\omega_0^2 = \frac{V_0}{b^2 M} = \frac{Ga^2}{Mh} \quad (5)$$

- the internal viscous relaxation time

$$\tau = \frac{\eta}{G}. \quad (6)$$

Setting:

$$\begin{aligned} \tilde{x} &= x/b; & \tilde{t} &= \omega_0 t \\ \tilde{K} &= K/K_0; & K_0 &= V_0/b^2 \\ \tilde{v} &= v/v_0; & v_0 &= b\omega_0 \end{aligned} \quad (7)$$

we rewrite equation (1) as:

$$\frac{d^2\tilde{x}}{d\tilde{t}^2} + \Gamma\frac{d\tilde{x}}{d\tilde{t}} + \sin\tilde{x} + \tilde{K}\big(\tilde{x} - \tilde{\rho}(\tilde{t})\big) = 0 \quad (8)$$

where $\Gamma = \omega_0\tau$.

We will from now on drop the tildas for simplicity. It is immediately clear that, in the absence of external driving, the dynamics of the joint depends on the single parameter $\Gamma = (\omega_0\tau)$, which measures the level of *internal* damping of the joint.

Two regimes can be clearly distinguished, namely the overdamped ($\Gamma \gg 1$) and the underdamped ($\Gamma < 1$) one.

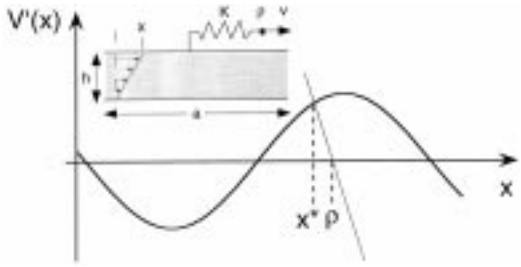

Fig. 1. Determination of the equilibrium displacement of the upper surface of the junction, x^*, for position ρ of the external driving point, for the setup schematized in the inset. $V'(x)$ is the pinning force, the slope of the straight line is the external stiffness.

3 The overdamped regime: $\Gamma \gg 1$

Inertia can be neglected, and, as long as the driving velocity is small enough (see below), the system equilibrates quasi adiabatically, *via* rapid viscous damping, in the instantaneous potential:

$$U(x,\rho) = -\cos x + \frac{K}{2}(x-\rho)^2. \tag{9}$$

The joint displacement $x^*(\rho)$ is determined by $\partial_x U = 0$, *i.e.* is obtained by intersecting $(\sin x)$ with the straight line $(-K(x-\rho))$ – see Figure 1. Let us now concentrate on the case where the external end of the spring is pulled at constant velocity:

$$\rho = vt. \tag{10}$$

Two situations are possible, depending on the value of the reduced spring stiffness as compared with the maximum reduced stiffness of the pinning potential: $K_m = K_0^{-1}\max(|d^2(V/V_0)/dx^2|) = 1$.

3.1 K > 1

The intersection is unique, and moves smoothly towards increasing x^* as ρ increases. The friction force, due to the viscous drag, is of order $\Gamma v(dx^*/d\rho)$. It vanishes smoothly with the pulling velocity.

The joint velocity $v(dx^*/d\rho) = vk/(k+\cos x^*)$ oscillates periodically about the pulling velocity without vanishing. Sliding is smooth, no stick-slip occurs.

One easily checks that the quasiadiabatic approximation is valid as long as the physical velocity remains much smaller than $v_1 = b/\tau$. At larger pulling velocities, the viscous drag force must be computed directly from the solution of the inertialess version of equation (8).

3.2 K < 1

As seen in Figure 2, as K decreases below 1, ranges of values of ρ develop in which the sinusoid and the loading straight line exhibit multiple intersections. The smaller K, the more numerous the solutions of the instantaneous equilibrium equation.

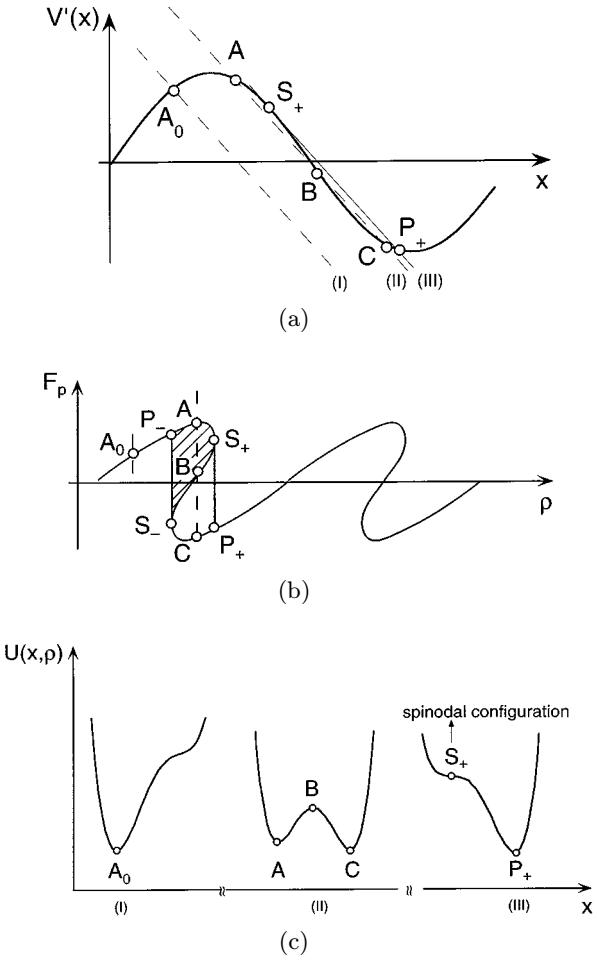

Fig. 2. (a) Local equilibrium construction for $K < 1$. The system exhibits a small range of multistability. When driven towards increasing x, it remains on branch (A_0A) up to the spinodal point S_+. (b) Corresponding pinning force $F_p(\rho)$. The shaded part of the hysteresis loop is the energy dissipated when moving by $\Delta\rho = 2\pi b$. (c) Total energy $U(x)$ for values of ρ corresponding to cases (I), (II), (III) of Figure 2a.

(a) Let us first consider the case where K is only slightly smaller than 1 (Fig. 2a). For $(2n+1)\pi - \delta\rho_s < \rho < (2n+1)\pi + \delta\rho_s$, with $\delta\rho_s \approx (2^{3/2}/3)(1-K)^{3/2}$, there are three such intersections. The system is *multistable* over the corresponding ranges of ρ values, in these ranges the pinning force opposing the pulling one,

$$F_p(\rho) = \sin x^*(\rho)$$

is multivalued (see Fig. 2b). The reentrant branch S_+BS_- in Figure 2b corresponds to unstable equilibrium positions. The other two branches describe locally stable equilibria. In the noiseless system considered here, no jump above the energy barrier of the total potential $U(x,\rho)$ (Fig. 2c) is possible.

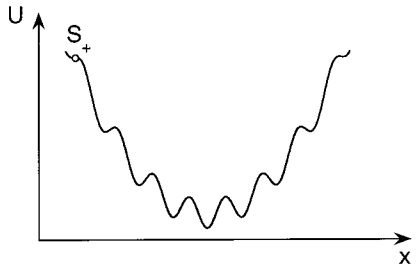

Fig. 3. Total energy $U(x)$ in the highly multistable case $K \ll 1$, drawn for $\rho = 0$, $K = 0.04$.

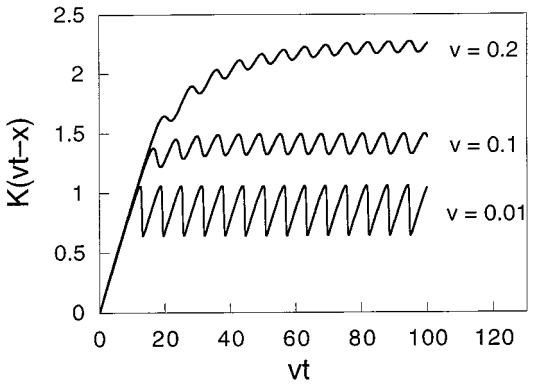

Fig. 4. Reduced external loading force $K(vt-x)$ *versus* $\rho(t) = vt$ for an overdamped junction with $\Gamma = 10$, $K = 10^{-1}$. The motion evolves continuously from atomic stick-slip for $v \ll 1$ to modulated sliding.

So, when the system is pulled to the right at vanishingly small velocity, its representative point follows branch (+) of the hysteretic $F_p(\rho)$ curve, up to the point S_+, where $\rho = \rho_{s+} = (2n+1)\pi + \delta\rho_s$, and the pinning force $F_p(\rho_s) = (1-K^2)^{1/2}$. At this point, the (+) minimum of $U(x,\rho)$ (Fig. 2c) vanishes – a spinodal instability occurs – and the overdamped system jumps rapidly into the closest stable minimum P_+. This scheme is exactly analogous to that analyzed for a real contact between two asperities, by Caroli and Nozieres [6].

The energy dissipated when moving over a period, $2\pi b$, of the pinning potential V, is the area of the hysteresis cycle shown in Figure 2b or, equivalently, the discontinuity ΔU_{eff} of the effective potential $U_{eff}(\rho) = U(x^*(\rho),\rho)$ at the spinodal point.

The corresponding motion may be termed stick-slip, since it is composed of alternating quasi-sticks, during which the system is steadily pulled by the spring out of a well of the pinning potential V, and slips which occur when the corresponding metastable equilibrium becomes unstable. It is during these fast jumps into the next stable equilibrium position that dissipation occurs.

Note, however, that the amplitude of these slips, $\approx 2\pi b$, lies in the subnanometric range, so that they should not be observable in practice, and what will be measured in such a regime is the *average* dynamical friction force, given, in this very low velocity regime, by:

$$F_d^0 = \bar{F}_p(v \to 0) = \frac{\Delta U_{eff}}{2\pi b} = \left(1-K^2\right)^{3/2}. \qquad (11)$$

So, the elastic multistability results in a finite value of the low velocity dynamic friction. This is to be compared with the static threshold

$$F_s = F_p(\rho_s) = \left(1-K^2\right)^{1/2}. \qquad (12)$$

Note that both values depend on the spring stiffness, the value of which controls the strength of the elastic hysteresis.

This regime holds as long as the time t_J necessary to "jump" from the saddle point S_+ down to the stable equilibrium point P_+ is smaller than the time for the spring to sweep the system at velocity v by the jump length, $\approx (1-K)^{1/2}$. Estimating the jump time as was done in reference [6], we find $t_J \approx (\Gamma^2/vK)^{1/3}$, we conclude that the imperfect stick slip described above should persist up to $v \approx v_1(K) \approx (1-K)^{3/4}/\Gamma$ (*i.e.* to physical velocities of order $(1-K^2)^{3/4}(b/\tau)$).

For higher velocities, once the system has been driven up to the spinodal configuration, it starts sliding and never "resticks" again in any potential well, as energy is fed in at a rate large enough to compensate viscous damping. As in the $K > 1$ case, its velocity is smoothly modulated about v, the amplitude of the modulation of course decreases as the pulling velocity increases.

(b) When K decreases, the number of extrema of the instantaneous potential U increases (see Fig. 3). For $K \ll 1$ – which, as we shall see in the next section, is the case in boundary lubrication experiments – U is very highly multistable. Nevertheless, the dynamical behaviour remains qualitatively similar to that described for case (a), namely, in the stick-slip regime found at $v < v_1(K) \approx K^{1/2}/\Gamma$, the fast slip brings the system into the potential well immediately next to the spinodal point ($\Delta x \approx 2\pi$)[1].

This overdamped dynamics is illustrated for $K = 0.1$, $\Gamma = 10$, in Figure 4. The corresponding average dynamical friction force is plotted in Figure 5.

In conclusion, our model predicts that when an overdamped junction is driven at constant velocity through a compliant spring, after being initially loaded up to its static threshold, it performs a modulated motion which evolves *continuously* between:

- strongly dissymetric "stick-slip" oscillations of molecular amplitude at very low velocities;
- regular sliding with a velocity very slightly modulated about the pulling one.

The K-dependent, finite, $v \to 0$ limit of the dynamical friction force *averaged* over many oscillations F_d^0 decreases from 1 to 0 as K increases from 0 to its critical value 1. $\bar{F}_d(v)$ then increases with v and goes asymptotically to its viscous limit $F_d^{visc}(v) = \Gamma v$ (see Fig. 5). Note that the convergence towards this limit is relatively slow.

[1] In the language of Josephson junctions, the phase slippage is by only one fluxon.

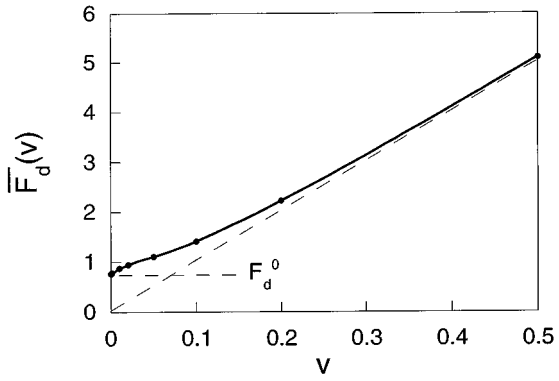

Fig. 5. Average friction force $\bar{F}_d(v)$ for an overdamped system with $\Gamma = 10$, $K = 10^{-1}$.

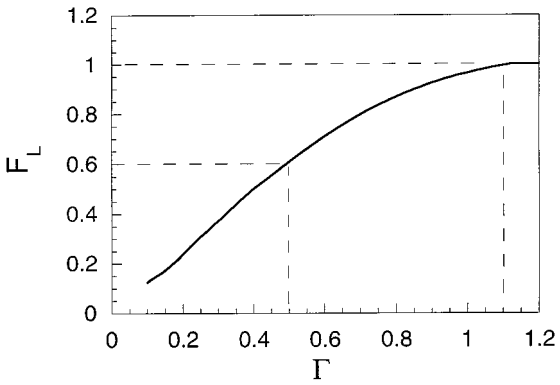

Fig. 6. Lower limit of the range of coexistence of the pinned frozen state and the shear molten one, *versus* internal damping coefficient Γ, as obtained from the data of reference [18].

4 The underdamped regime: $\Gamma < 1$

In this regime, the system develops a qualitatively different dynamical behavior. Namely, when driven by a constant applied (non dimensional) force F, it exhibits *dynamical hysteresis*.

(a) For $F > F_M = 1$, equilibrium is impossible, the system slides steadily.

(b) For $F < 1$, it can sit in one of the equivalent stable equilibrium positions $x_{st}(F) = \sin^{-1} F + 2p\pi$. However, numerical [18] and, later, analytical [19] investigations have shown that, for $\Gamma < 1.1$, in a finite range of values of σ: $F_L < F < F_M = 1$, this equilibrium solution coexists with another, "running" one, in which the system slides continuously with a periodically modulated, finite velocity[2]. That is, in this hysteretic range, there are two dynamical attractors, the basins of attraction of which, in the phase space $(\dot{x}, x)$, have been studied in detail by Imry and Schulman [19]. Which of them is reached after the initial transient depends on the initial conditions: if the system is launched with a large enough energy, since damping is small, the input from the drive is able to compensate for the dissipation, allowing the system to run away permanently. For lower initial energy, on the contrary, it relaxes down into one of the pinning wells.

This behavior, observed in the low temperature hysteretic Josephson junctions, is precisely what has been found numerically by Thompson and Robbins [12], and by Persson [13], in their simulations. One may check that these were indeed performed with parameters corresponding to our underdamped regime ($\Gamma < 1$).

The width of the hysteretic range – the range of coexistence of the pinned frozen state and of the shear-molten one – decreases with increasing Γ: F_L increases from 0 (for $\Gamma \to 0$) to 1, for $\Gamma = 1.1$. A numerical plot of $F_L(\Gamma)$, extracted from the data of reference [18], is shown in Figure 6. We show in Figure 7 the schematic shape of the hysteretic F *versus* $\langle \dot{x} \rangle$ curve, for a system with damping coefficient $\Gamma = 0.5$, driven by a constant force (infinitely compliant spring limit). $\langle \dot{x} \rangle$ is the time averaged velocity in the running state.

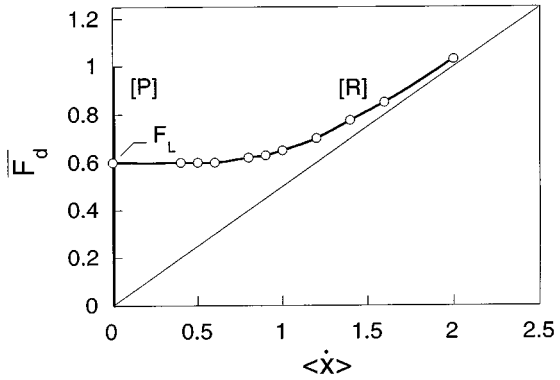

Fig. 7. Average friction force in the molten (running) state (branch R) and in the pinned frozen state (branch P) for an underdamped junction with $\Gamma = 0.5$. The range of dynamic bistability extends from $F_L \approx 0.6$ to 1.

We now want to analyze how this underdamped system responds to pulling at constant velocity v through a spring of finite compliance K. The initial loading phase, in which the pinned system is pulled from its initial equilibrium position $x = 0$ up to the spinodal threshold S_+, where shear melting occurs, does not differ from that for the overdamped case. But, once sliding starts, since the internal damping time $(\omega_0^2 \tau)^{-1}$ is now small with respect to the period of oscillation in a "pinning well", ω_0^{-1}, energy dissipation is slow. This results in the fact that the length of the slip, at the end of which the system gets pinned again, varies substantially with the values of the three parameters Γ, K, v.

For a detailed analysis of slip length and duration, we refer the reader to reference [17]. We only reproduce here the most salient features of the results obtained by these authors:

- for $K > K_m = 1$, the only stationary regime is modulated sliding. As in the overdamped case, there is no static threshold, dynamical friction is viscous.

[2] This is the relevant regime for Josephson junctions at low temperature. It has been identified and studied experimentally in that context.

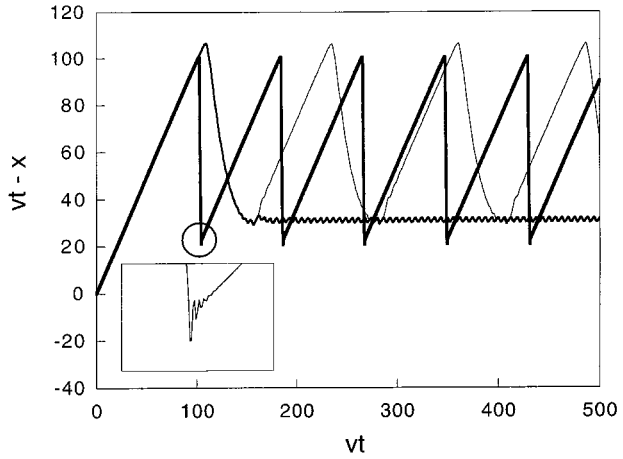

Fig. 8. External spring elongation for an underdamped junction ($\Gamma = 0.24$) driven by a weak spring ($K = 10^{-2}$) at various velocities. Inset shows the detail of underdamped oscillation in the pinning well at the end of a slip. At low velocity ($v = 5 \times 10^{-2}$; thick line), periodic stick-slip occurs. Between $v = 0.82$ (thin line) and $v = 0.83$ (medium thick line) the motion bifurcates to modulated sliding.

- for $K < 1$, the velocity regimes must be classified according to the respective values of v and $v_0 = 2\pi N/T_N$, where N and T_N are the (reduced) length and duration of the slip.

(i) When $\Gamma^2 \ll K \ll 1$, at low velocities, the system performs periodic motion the basic unit of which is composed of a *stick* period followed by several slowly attenuated large oscillations. In these "*bouncing slips*" the representative point, starting from S_+, overshoots the lowest well of the total potential U (see Fig. 3) and bounces a few times across the modulated parabola before damping drives it into one of the pinning wells, where it gets slowly refrozen. We will see that, in practice, this regime is irrelevant to existing experiments.

(ii) For $K < \Gamma^2 < 1$ the system, while *underdamped* when relaxing inside a pinning well, is *overdamped* when it is depinned and slips. At low velocities, it performs regular stick-slip. The slip length depends on the relative values of K and Γ Clearly, it increases when damping and/or stiffness decrease. The duration of the slip is roughly Γ/K. As v increases, so does the time for escaping from the spinodal region, since, due to the drive, the spinodal region itself slips in the jump direction. At a critical velocity v_c the drive overcomes the damping before repinning can take place: the motion bifurcates *discontinuously* from stick-slip to modulated sliding.

(iii) For $v > v_c$, the system settles in the running (periodically modulated sliding) state.

This behavior is illustrated numerically in Figure 8, for $K = 10^{-2}$, $\Gamma = 0.24$, and several values of the reduced velocity v. The oscillations shown in the insert correspond to the underdamped bounces within one pinning well. The slip length Δx_{sl} is on the order of 12 periods of the pinning potential, much larger than in the overdamped regime.

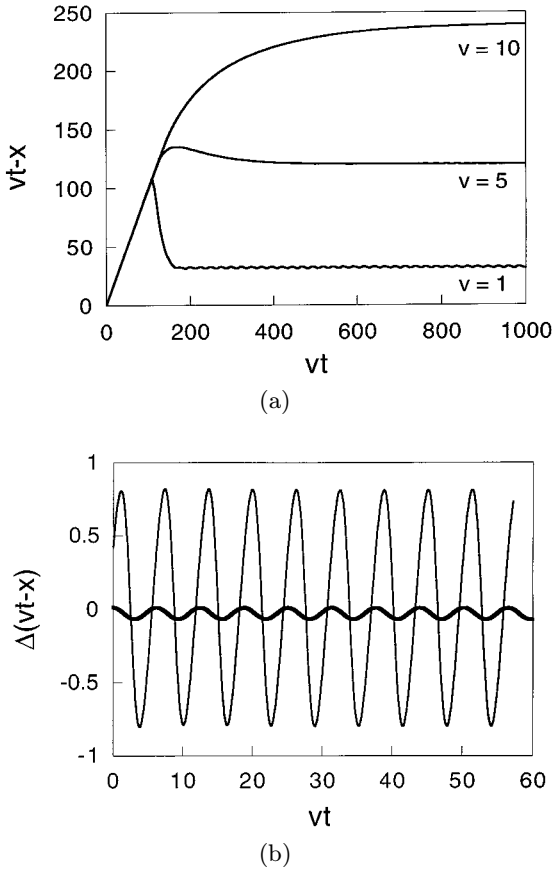

Fig. 9. (a) Same as Figure 8 for large velocities. The level of dynamic friction increases, leading to gradual disappearance of the stiction spike. (b) Decrease of the modulation amplitude in the sliding state with increasing v (thin: $v = 1$; thick: $v = 5$).

The delay in the beginning of the slip due to the competition between the crossing of the spinodal instability and the drive results in a slight increase of the maximum force ("static threshold"), while its minimum value increases by a comparable amount. At the end of the slip the system is captured within a pinning well which comes closer to the spinodal as v increases. The period of the stick-slip, essentially controlled by the stick time, scales roughly as V^{-1}.

For these values of K and Γ, the critical velocity v_c at which stick-slip disappears abruptly lies between 0.82 and 0.83. As v is increased slightly above v_c, the initial transient exhibits a "stiction peak", the shape of which is practically identical with the first stick-slip immediately below v_c. In this sliding regime, the average stationary dynamical friction force remains practically constant up to $v \approx 1$, then increases with v (see Fig. 9a) while the force modulation decreases (Fig. 9b). For $v = 10$, $\bar{F}_d(v)$ is practically equal to its asymptotic viscous value Γv. This rise of the stationary force level leads to the gradual disappearance of the stiction peak. Note that the height of this peak – corresponding to the static threshold, remains

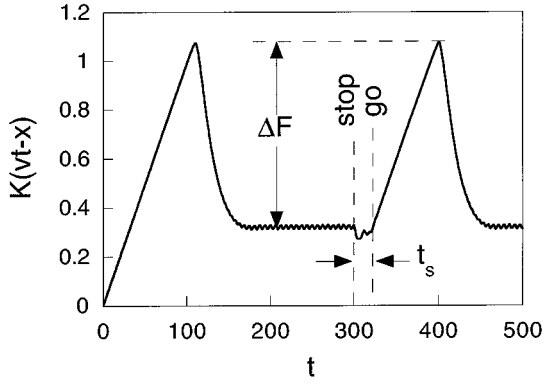

(a)

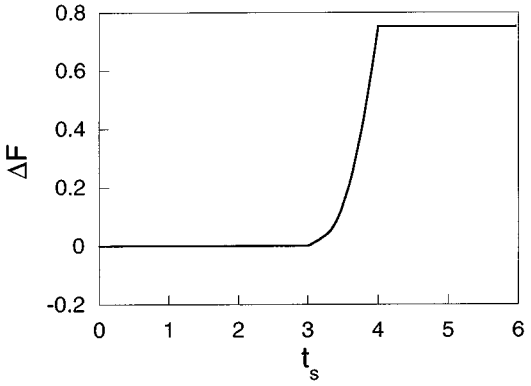

(b)

Fig. 10. (a) Simulation of a stop and go experiment: the underdamped system ($\Gamma = 0.24$, $K = 10^{-2}$) is driven at constant velocity $v = 1$ from rest into modulated sliding. The drive is stopped at $t = 300$, and resumed at $t = 300 + t_s$. Here ($t_s = 20$) repinning during the stop phase leads to a second stiction spike of reduced height ΔF. (b) Height of the second stiction spike ΔF *versus* stopping time t_s.

practically constant (of order 1 in our reduced units), all through this evolution.

This scenario is robust against variations of the stiffness. Decreasing K down to 5×10^{-5} leads to practically unchanged force maxima and minima. Accordingly the slip length scales as K^{-1}. The critical velocity decreases very slowly with K. For $K = 5 \times 10^{-5}$, $v_c \approx 0.3$. The dynamic friction force $\bar{F}_d(v)$ in the steady sliding state, above v_c, remains quasi-constant up to $v \approx 1$ whatever K. This can be understood easily with the help of Figure 7: above the bifurcation, the system, after the initial depinning transient, gets trapped into the running state, where the friction force is constant (up to the small modulations shown in Fig. 9b). So, $\bar{F}_d(v)$ is practically identical with the curve $F(\langle \dot{x} \rangle)$ describing the "running state" branch of the hysteretic response to a constant shear force. On this branch, the force remains very close to its zero velocity limit F_L, roughly of order Γ (see Fig. 6), up to the crossover with the bare viscous curve, which therefore always occurs in the range $v \approx 1$. This fixes the upper limit of the velocity range in which the system can be said to slide under constant dynamic stress.

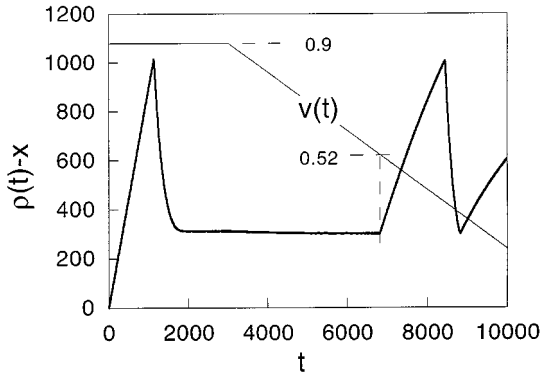

Fig. 11. Reduced spring elongation *versus* time for the loading protocol $\dot{\rho}(t)$: for $t < 3000$, $v = 0.9$. For $t > 3000$, $v(t) = \dot{\rho}$ is ramped down linearly with $\dot{v} = -10^{-4}$. The system remains in the metastable molten state down to $v = 0.52$.

Finally, decreasing Γ leaves this description unchanged, apart for a global scaling of velocities by a factor on the order of Γ^{-1}.

We have also simulated numerically "stop and go" experiments [9]. In the case displayed in Figure 10a, the system has been driven at the constant velocity $v = 1$ until it settled in the quasi-steady sliding regime. At $t_0 = 300$, the driving was stopped, then resumed (with the same $v = 1$) at $t_1 = t_0 + \Delta t_{stop}$, with $\Delta t_{stop} = 20$. During the stopping time, the system relaxes into the pinned state, so that, when driving is restarted, the system must overcome a stiction peak which is practically equal to the initial one. Of course, the second peak only appears when the stopping time is larger than the typical energy relaxation time, $\approx \Gamma^{-1}$, of order 4 in the case shown in Figure 10b.

Finally, another question to be considered is concerned with the above mentioned specificity of the underdamped regime, namely dynamical hysteresis and the possibility of observing it directly. In this perspective, we have studied the following numerical protocol (Fig. 11): the system is set into steady sliding motion (in the case shown, at a velocity just above v_c). Then, the driving velocity is slowly ramped down linearly. We find that it remains in the sliding state (the "running state" of Ref. [17]) down to a velocity v_{min} much smaller than v_c (≈ 0.8), where it finally flips back into the stick-slip regime. We find that v_{min} decreases slowly – the width of the hysteretic range increases with decreasing stiffness K (for example, $v_{min}(K = 10^{-2}) \approx 0.6$).

However, even for $K \approx 10^{-3}$, this width remains much smaller than that calculated for driving at constant external force. This is to be attributed to the fact that, at a given v, the modulations of the sliding trajectory in phase space are found to increase with the stiffness of the pulling spring. The system flips back into the pinned state preliminary to stick-slip as soon as its trajectory crosses the separatrix between the two regimes. As v is reduced, this

occurs all the sooner that the modulation amplitude is larger. So, the hysteresis range shown in Figure 7 should be considered only, in our mechanical case, as a theoretical limit corresponding to an infinitely compliant driving system.

5 Discussion

We must now confront the results of the above analysis with the existing experimental data on junctions lubricated with small molecules.

Let us first consider the results of Israelashvili and coworkers concerning the sliding dynamics under driving at constant velocity, with ultra thin films (typically, two molecular layers) of OMCTS and hexadecane [9].

The qualitative dynamical scenario which they observe is identical with that corresponding to the moderately underdamped regime of our lumped junction model, described in the preceding section. Namely, up to $v = v_c$, periodic stick-slip prevails. At v_c, stick-slip disappears discontinuously, and steady sliding sets in. In a moderate velocity range above v_c, an initial stiction peak is observed, and the measured dynamical friction force (corresponding to our average $\bar{F}_d$) is quasi v-independent, and equal to the minimum value of F at the end of the slip. Erratic stick-slip is often observed in a narrow v-range above v_c. We will come back to this below.

Using the results of Section 4, we evaluate the internal damping parameter Γ from the measured values of F_{min}/F_{max} in stick-slip. This, according to our model, is, up to small corrections due to the weak variations of the static force threshold with v, equal to the reduced value of F_L (the reduced value of the low-v dynamic force on the running branch). Knowing F_L, we deduce Γ from the master curve (Fig. 6). From Figures 7 and 12 of reference [9], we evaluate:

- for OMCTS, $\Gamma \approx 0.5$;
- for hexadecane, $\Gamma \approx 0.45$.

Since these are only rough orders of magnitude, we will take as an indicative value for these experiments $\Gamma = 0.5$.

On the other hand, our reduced stiffness parameter is measured in units of $(M\omega_0^2) \approx F_{max}/b$. In the experiments, $F_{max} \approx 10$ mN, the machine stiffness is of order 500 N/m, the mass $M = 20$ g. Assuming the period $(2\pi b)$ of the pinning potential to be of order 0.3 nm – a value suggested by the structure of the mica cleavage plane, we get $K \approx 2 \times 10^{-6}$. For these K and Γ, we calculate that, in physical units:

$$v_c \approx 0.25\omega_0 b = 0.25(F_{max}b/M)^{1/2} \qquad (13)$$

which yields a critical velocity of about $1\,\mu$m/s, *i.e.* of the order of those observed for OMCTS and hexadecane. Note that (13) has the form of the expression proposed by Thompson and Robbins [12]. Our model thus predicts that their numerical constant C, here equal to 0.25, is in fact a slowly decreasing function $C(K, \Gamma)$ of both the reduced stiffness K and the internal damping parameter Γ.

With the same parameters, we obtain: $\omega_0 \approx 10^4$ rad/s, from which we estimate $\tau \approx 5 \times 10^{-5}$ s, and, on the basis of our above stop and start simulation, a refreezing time $\Delta t_{fr} \approx (\omega_0\Gamma)^{-1}$ of order 2×10^{-4} s. That is, we find that the delay before refreezing should be much too small to be observable. This is indeed the case for OMCTS – but such an argument is, of course, only of the noncontradictory kind. For hexadecane, observed refreezing times are of the order of seconds – that is, hugely larger than the above estimate. This leads us back to analyzing the physical assumptions implied by ansatz (2). Guided by the idea of "refreezing on the spot", and by the fact that the mica confining plates are atomically quasi perfect, we have assumed that the conservative part of the average friction force has a strong (periodic) non linearity. On the other hand, we have assumed for simplicity, in the absence of further information, that the dissipative part is both linear and non retarded. Both these approximations become doubtful in the case of chain molecules such as hexadecane: indeed, there are all reasons to believe that sliding at high enough velocity may induce conformational changes and/or further ordering under shear – a phenomenon observed for this material during initial loading. Such processes, if present, lead to important non Newtonian effects and to the possibility that internal viscous relaxation becomes much more strongly retarded. If this is the case, our model in its present simple version is certainly insufficient for such materials.

In view of the possibility that slower processes might become relevant in sliding, it would be interesting to check whether the refreezing time exhibits any dependence on the duration or length of sliding prior to stopping.

Let us now come back to our second important simplification – the neglect of noise. The effect of introducing white noise into equation (1) has been studied by Ambegaokar and Halperin [20] in the overdamped case, and by Ben Jacob, Bergmann and Schuss [21] in the underdamped, hysteretic one[3].

Noise enables the system to perform activated jumps above energy barriers. In the overdamped case, this entails that "premature" jumps out of metastable equilibrium occur with a finite probability. The system can slip before reaching the spinodal point. This results in the development of irregularity of the stick-slip motion, which should show in particular through a dispersion of the static force threshold[4].

In the underdamped case, one expects a more spectacular effect. Indeed, the noise activated jumps are now able, in the range of dynamic bistability, to activate jumps

[3] Note, however, that these authors concentrate mainly on calculating the effect of noise on the average voltage associated with a given current in the Josephson junction, the equivalent of which, for our problem, would be the average velocity at strictly constant stress, a quantity which is not directly accessible in friction experiments.

[4] Such effects could be responsible for the self-accelerating drift effects observed by Reiter *et al.* [22] following a sudden jump of the maximum applied shear force up to a value close below the static threshold.

between the pinned and the running state. This results in the system spending on average, in this range, a finite fraction of the time in each state. The fraction spent, *e.g.*, in the running one, increases from 0 to 1 as the average reduced force level increases from F_L to 1.

In practice, under loading at constant velocity through a spring, this should give rise, above v_c, to a regime with a random alternation of sliding periods separated by a repinning event followed by reloading, *i.e.* by a stiction peak. This is precisely what is observed in experiments as erratic stick-slip. It would therefore be of interest to study how the average recurrence time of the stick-slip events, in this regime, varies with v/v_c.

Of course, such a phenomenon may also result from non-intrinsic, experimental noise. This brings up the question of the level of the intrinsic noise. Close to equilibrium under zero shear, this is related to the internal viscosity η by the fluctuation dissipation theorem. However, no such a systematic relation holds for the out of equilibrium system. This points to the interest of developing a more microscopic model of the junction dynamics, in the spirit of the studies of the dynamics of the Frenkel-Kontorova model and randomly pinned charge density waves [22].

It is reasonable to expect the noise level to increase when the layer approaches melting, as is suggested by the strong increase in stick-slip irregularities found numerically by Thompson and Robbins [12].

Direct information can only be obtained either from such realistic simulations, or from experiments. In the sheared pinned state (*i.e.* below the static threshold), this would mean measuring the a.c. *linear* visco elastic response of the junction *under finite d.c. shear.* In practice, this could be performed by superimposing a low and a high frequency driving excitation. The noise level would then be obtained *via* the fluctuation-dissipation relation.

Up to now, we have focussed our discussion on experiments concerning the dynamical behavior under driving at constant velocity. Although these provide enough data for a reasonable check of the model, it would be desirable to get fuller confirmation by proceeding as suggested in Section 2. Namely, in principle, ω_0 and τ could be obtained directly from the measurement of the elastic and loss moduli in an linear a.c. reponse experiment.

Several such experiments have been performed by Granick *et al.* [11,16,23] Those in which the layer behaves, at small strain, as a viscoelastic solid, appear all to pertain to the regime of strong internal overdamping (typically, we estimate Γ values of the order of 10^2 at least), in contradistinction with the conditions prevailing in the work of Israelashvili *et al.* This difference is certainly assignable to the fact that the two sets of experiments have been performed at quite different levels of normal load L (typically more than 10 times lower in the a.c. conditions than in the sliding ones). We are therefore unable, for the moment, to connect both sets of data. Clearly, it would be very useful that the two sets of measurements be performed on one same sample under the same conditions, in particular the same normal load. The orders of magnitude of Γ and ω_0 evaluated above suggest that, for these underdamped systems, it would be necessary to work in the kHz frequency range in order for loss effects to be safely measurable.

This leads us to one further remark concerning normal load effects within the underdamped regime itself. We just noticed that, for a layer of given thickness, Γ appears to be L-dependent. Most probably, the same is true of the pinning strength and, hence, of the reduced stiffness. This will result in an L dependence of the reduced critical velocity – *i.e.* of the constant $C(K,\Gamma)$ appearing in expression (13). This should be kept in mind when analyzing v_c *versus* L data.

Finally, one might imagine to try and evaluate the degree of validity of our assumption of a perfectly periodic pinning potential by looking for parametric resonances giving rise to force jumps analogous to the Josephson steps [24]. These have been studied by Helman *et al.* [25] for our mechanical system. This would mean superimposing to a steady drive at mean velocity $v > v_c$ a velocity modulation at frequencies multiples of $2\pi b/v$, *i.e.* in the kHz range.

In summary, we have proposed here a simple phenomenological model for highly confined, ultra-thin layers of small lubricant molecules. Though schematic, it accounts correctly for all the qualitative features of the sliding dynamics as studied by Israelashvili *et al.*, and is compatible with their quantitative measurements. It emerges from our discussion that these d.c. investigations all deal with layers in the regime of moderate internal underdamping – hence their dynamic bistability. On the contrary, the a.c. responses studied by Granick *et al.* are concerned with the opposit, strongly overdamped (hence monostable) regime.

Performing both types of experiments under the same conditions would provide a firmer benchmark for a model which, if legitimate, could be used as a basis for further progress towards bridging between nanotribology and friction on a larger scale.

Appendix

In the (resistively shunted) lumped circuit model [17,24], the basic equation describing the time evolution of the voltage drop V across a Josephson junction driven by a current I is:

$$C\dot{V} + \frac{V}{R} + I_J \sin\theta = I \tag{A.1}$$

$$V = \Phi_0 \dot{\theta}, \tag{A.2}$$

C is the capacitance of the junction, R its normal resistance, I_J the Josephson current amplitude, Φ_0 the flux quantum, θ the order parameter phase difference across the junction.

This junction may be part of a superconducting loop of self-inductance L which, in the presence of an external magnetic field, encloses a flux Φ_{ext}.

The correspondence between the parameters standardly used in the Josephson problem and ours is the following table.

Josephson	Friction
phase: θ	upper surface reduced position: x/b
capacitance: C	mass: M
inverse resistance: R^{-1}	$\eta a^2/h$
$L_J = (I_J/\Phi_0)^{-1}$	$(V_0/b^2)^{-1}$
Josephson frequency: ω_J	ω_0
$\tau_m = L_J/R$	τ
$K = L_J/L$ (L = external self inductance)	$\tilde{K} = K/K_0$
$\Phi_{ext}(t)/\Phi_0$	$\rho(t)/b$

References

1. *Physics of Sliding Friction*, edited by B.N.J. Persson, E. Tosatti, NATO ASI Series, Series E: Applied Sciences, **311** (Kluwer, Dordrecht 1996).
2. B.N.J. Persson, *Sliding Friction; Physical Principles and Applications*, Nanoscience and Technology Series (Springer Verlag, Berlin, 1998).
3. F. Heslot, T. Baumberger, B. Perrin, B. Caroli, C. Caroli, Phys. Rev. E **49**, 4973 (1994); T. Baumberger, in Ref. [1], p. 1; J.H. Dieterich, J. Geophys. Res. **84**, 2161 (1979); B.D. Kilgore, M.L. Blanpied, J.H. Dieterich, Geophys. Res. Lett. **20**, 903 (1993).
4. P. Berthoud, T. Baumberger, Proc. Roy. Soc. Lond. A, in press (1997).
5. T. Baumberger, L. Bureau, E. Falcon, to be published.
6. C. Caroli, P. Nozières, in Ref. [1], p. 27; C. Caroli, P. Nozières, to be published.
7. J.N. Israelashvili, Surf. Sci. Rpt **14**, 109 (1992).
8. J.M. Georges, A. Tonck, J.-L. Loubet, D. Mazuyer, E. Georges, F. Sidoroff, J. Phys. II France **6**, 57 (1996).
9. H. Yoshizawa, J.N. Israelashvili, J. Chem. Phys. **97**, 11300 (1993).
10. A.D. Berman, W.A. Ducker, J.N. Israelashvili, in Ref. [1], p. 51.
11. G. Reiter, A.L. Demirel, J. Peanasky, L. Cai, S. Granick, J. Chem. Phys. **101**, 2606 (1994).
12. P.A. Thompson, M.O. Robbins, Science **250**, 792 (1990); M.O. Robbins, P.A. Thompson, Science **253**, 916 (1991).
13. B.N.J. Persson, Phys. Rev. Lett. **71**, 1212 (1993).
14. J.M. Carlson, A.A. Batista, Phys. Rev. E **53**, 4153 (1996).
15. M.G. Rozman, M. Urbakh, J. Klafter, Phys. Rev. E **54**, 6485 (1996).
16. A.L. Demirel, S. Granick, Phys. Rev. Lett. **77**, 2261 (1996).
17. E. Ben Jacob, Y. Imry, J. Appl. Phys. **5**, 4317 (1980).
18. C.M. Falco, Am. J. Phys. **44**, 733 (1976); D.E. McCumber, J. Appl. Phys. **39**, 3113 (1968).
19. Y. Imry, L.S. Schulman, J. Appl. Phys. **49**, 749 (1978).
20. V. Ambegaokar, B.I. Halperin, Phys. Rev. Lett. **22**, 1364 (1969).
21. E. Ben Jacob, D.J. Bergman, Z. Schuss, Phys. Rev. B **25**, 519 (1982).
22. L. M. Floria, J.J. Mazo, Adv. Phys. **45**, 505 (1996).
23. G. Reiter, A.L. Demirel, J. Peanasky, L. Cai, S. Granick, in Ref. [1], p. 119
24. See for example, D.R. Tilley, J. Tilley, *Superfluidity and Superconductivity*, Graduate Student Series in Physics (Adam Hilger Ltd, Bristol, 1986); K.K. Likharev, *Dynamics of Josephson junctions and circuits* (Gordon and Breach, Philadelphia, 1986).
25. J.S. Helman, W. Baltensperger, J.A. Holyst, Phys. Rev. B **49**, 3831 (1994).